APL Materials

A new perspective on lone pair dynamics in halide perovskites

Cite as: APL Mater. **8**, 050902 (2020); https://doi.org/10.1063/5.0001908
Submitted: 20 January 2020 . Accepted: 01 May 2020 . Published Online: 14 May 2020

Richard C. Remsing, and Michael L. Klein

A new perspective on lone pair dynamics in halide perovskites

Cite as: APL Mater. 8, 050902 (2020); doi: 10.1063/5.0001908
Submitted: 20 January 2020 • Accepted: 1 May 2020 •
Published Online: 14 May 2020

Richard C. Remsing[1,a] and Michael L. Klein[2,b]

AFFILIATIONS

[1] Department of Chemistry and Chemical Biology, Rutgers University, Piscataway, New Jersey 08854, USA
[2] Institute for Computational Molecular Science and Department of Chemistry, Temple University, Philadelphia, Pennsylvania 19122, USA

Note: This paper is part of the Special Issue on New Perspectives on Emerging Advanced Materials for Sustainability.
[a] **Author to whom correspondence should be addressed:** rick.remsing@rutgers.edu
[b] mike.klein@temple.edu

ABSTRACT

Halide perovskites form the foundation of an emerging class of materials for broad application in renewable and sustainable applications, including photocatalysis and solar energy harvesting. These materials exhibit beneficial photophysical properties, including bandgaps suitable for solar energy harvesting and efficient charge screening that underlies efficient charge carrier separation and resistance to defects. For organic–inorganic hybrid perovskites, these benefits are thought to arise, in part, from dipolar molecular cations that can reorient in response to charged particles and defects. In this work, we provide a similar perspective for inorganic metal halide perovskites, which do not contain molecular species with permanent dipoles. We discuss how lone pair electrons lead to dipolar ions that exhibit dynamics in analogy with traditional molecular plastic crystals and hybrid perovskites. We argue that further understanding these electronic plastic crystal motions with first principles simulations and synchrotron scattering can help create a basic understanding of photophysical properties of metal halide perovskites and inform the design of advanced functional materials.

I. BACKGROUND

Metal halide perovskites of generic composition ABX_3 have garnered significant attention as advanced materials for renewable and sustainable energy applications.[1–3] For example, numerous halide perovskites show exceptional photovoltaic efficiency, promising improvements in solar cell technologies and use as components in photocatalytic devices.[3] The favorable optical and electronic properties of halide perovskites have created interest in their use in optoelectronics, such as light emitting diodes (LEDs).[2,4,5] Much work has focused on the structure and dynamics of hybrid organic–inorganic halide perovskites, composed of an organic cation at the A-site, a metal at the B-site, and halides at the X-sites. For example, methylammonium lead iodide, $NH_3CH_3PbI_3$ or $MAPbI_3$, is a highly studied member of this class of perovskites.[1–3,6]

Unlike simpler A-site cations, such as Cs^+, the MA^+ cation has a permanent dipole moment that can undergo thermally induced rotational motion.[7–12] Moreover, upon introduction of an excess charge into the lattice, e.g., an atomic defect site or an excess electron, these dipolar cations can readily reorient to polarize in response and screen the charge.[11,13] Such liquid-like screening is thought to underly the robustness of halide perovskites to defects because charged defects are readily screened by this polarization.[13–17] This screening is also suggested to result in the ability of halide perovskites to efficiently separate charge carriers from bound excitons, ultimately by "solvating" each diffuse charge, much like a polar solvent solvates and separates ions of opposite charge.[11,13–15,17] Both simulations and experiments have shown that these MA^+ dipoles have a rotational correlation time on picosecond timescales, leading to fast polarization of the perovskite material in response to charged excitations.[7–10]

Characterizing the dipolar structure and dynamics of organic–inorganic halide perovskites has created a foundation for understanding the variety of important photophysical properties of these

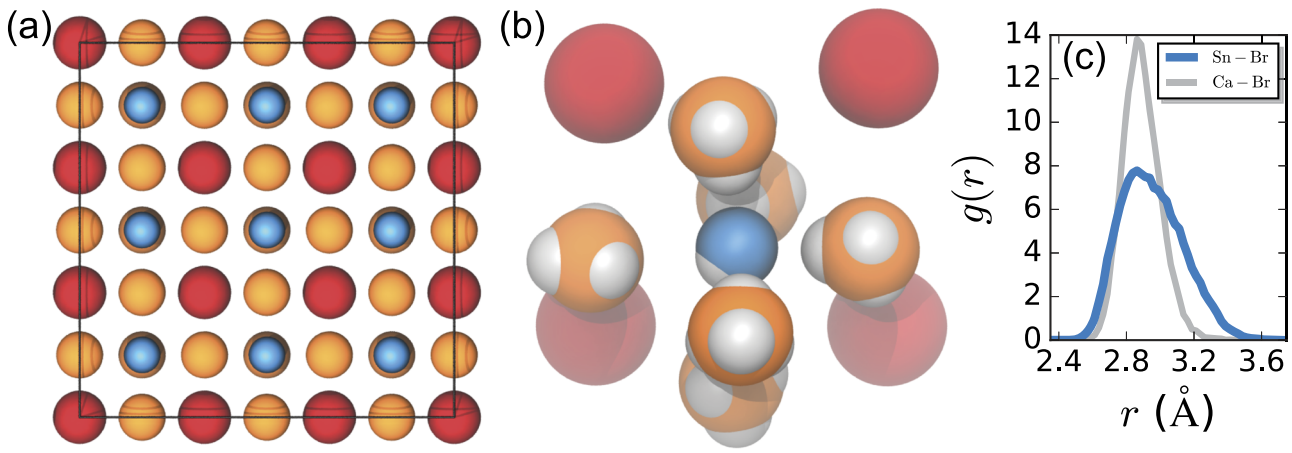

FIG. 1. (a) Snapshot of the structure of the cubic phase of $CsSnBr_3$. Red, blue, and orange spheres correspond to Cs, Sn, and Br. (b) Simulation snapshot showing MLWFCs (gray spheres) of Sn and Br, highlighting the off-centering of Sn caused by pointing its Sn-LP dipole toward a face of its octahedral coordination shell. (c) This off-centering manifest in an asymmetric first peak of the Sn–Br pair distribution function, $g(r)$, determined from AIMD simulations. Halide perovskites with symmetric B-site cations, such as $CsCaBr_3$, do not exhibit off-centering and result in a symmetric first peak of the Ca–Br $g(r)$.

materials. However, similar properties are observed for other halide perovskites with simpler A-site cations, such as $CsPbX_3$ and $CsSnX_3$, where X indicates Cl, Br, or I.[18–21] For example, inorganic halide perovskites can also have high dielectric constants and efficiently separate and solvate charges, much like the organic–inorganic hybrid perovskites. Moreover, both the simulation and experiment have identified large and fast (sub-ps) polarization fluctuations in this class of metal halide perovskites.[22] These observations suggest that $CsPbX_3$, $CsSnX_3$, and similar perovskites behave qualitatively analogous to those containing dipolar organic cations, despite the noticeable absence of a permanent dipole-containing molecular ion. This suggests that the permanent dipole of an organic cation is not solely responsible for the advantageous photophysical properties of halide perovskites, but instead, the inorganic framework can dominate the behavior of these materials.[18–21]

At ambient temperatures, $CsPbX_3$ and $CsSnX_3$ halide perovskites typically are in the cubic phase, shown in Fig. 1(a) for $CsSnBr_3$. However, Seshadri and co-workers have shown that the B-site ion is not located at the center of an octahedral coordination environment in the cubic phase, as one might expect.[23–27] Instead, Pb and Sn ions exhibit dynamic off-centering; the ion position fluctuates between eight energetically favorable asymmetric configurations. Ultimately, this off-centering stems from the s^2 lone pair of each of these cations and is not observed for symmetric B-site cations, as in $CsCaX_3$ perovskites. Localization of this lone pair (LP) results in a Pb-LP or Sn-LP dipole, and it is energetically unfavorable for the lone pair to point toward one of the surrounding X ions due to electrostatic repulsion, as shown in Fig. 1(b). These interactions push the B-site cation off-center, which manifests in the pair distribution function, $g(r)$, shown in Fig. 1(c), as predicted by simulations described in Sec. II. For $CsSnBr_3$, the Sn–Br $g(r)$ first peak is asymmetric due to the asymmetry of the off-center Sn ion. In contrast, halide perovskites with symmetric B-site cations without a significant dipole, such as $CsCaBr_3$, display a symmetric first peak in the Ca–Br $g(r)$ [Fig. 1(c)]. To minimize electrostatic repulsions between like charges, the Pb or Sn atom will move away from the center of its octahedral coordination shell and point its dipole toward one of the eight faces of the octahedron.

At temperatures large enough to cause cation off-centering, e.g., above the phase transition temperature to the cubic phase of $CsSnBr_3$,[24] thermal fluctuations activate rotational motions of the lone pairs in the system.[28] This type of electronic plastic crystal motion can be quantified by monitoring time correlations of relevant descriptors. For Sn-LP dipole rotational motion, a good descriptor is the normalized Sn-LP dipole moment vector. For Cs^+ or Br^-, each with four orientationally equivalent lone pairs, on average, the descriptor must account for the orientational symmetry of the local electronic structure. Recent work has used tetrahedral rotor functions to describe the orientational fluctuations of lone pairs around these ions,[28] taking inspiration from the examination of molecular plastic crystals.[29,30] Here, we discuss this perspective further and create an analogy between dipolar cations such as MA^+ and the Sn-LP dipoles in metal halide perovskites.

II. COMPUTATIONAL METHODS

We perform *ab initio* molecular dynamics (AIMD) simulations of halide perovskites using CP2K and the *QUICKSTEP* module.[31,32] We employ molecularly optimized (MOLOPT) Goedecker–Teter–Hutter (GTH) double-ζ valence single polarization short-ranged (DZVP-MOLOPT-SR-GTH) basis sets[32] with GTH-PADE pseudopotentials[33] to represent the core electrons. We explicitly treat the valence electrons using the PBE[34] functional with a plane wave cutoff of 400 Ry, as implemented in CP2K. This choice of functional enables connection to earlier work on similar systems.[24] We first equilibrated each system, consisting of a 3 × 3 × 3 supercell, at constant temperature using a Nosé–Hoover thermostat chain of length three[35,36] and the equations of motion were integrated with a timestep of 1.0 fs. We then equilibrated each system in

the microcanonical (NVE) ensemble. Production simulations, over which statistics were gathered, were performed in the NVE ensemble over a minimum of 10 ps of simulation time. The maximally localized Wannier function centers (MLWFCs) were computed using CP2K, wherein the MLWF spreads were minimized according to the formulation of Ref. 37.

We characterize the rotational dynamics of MLWFCs with two time correlation functions, discussed in previous work.[28] In order to quantify the Sn-lone pair dipole rotational motion, we present the rotational correlation function

$$C_{\mathrm{rot}}(t) = \langle P_2(\mu(t)\cdot\mu(0))\rangle, \tag{1}$$

where $\mu(t)$ is the Sn-MLWFC unit vector at time t and $P_2(x)$ is the second order Legendre polynomial. For Br atoms, we discuss the TCF of tetrahedral rotor functions, M_γ, of order $l = 3$, which have been used to characterize the rotational motion of tetrahedral structures in previous work on ionic crystals.[29] Here, γ labels the $(2l + 1)$ functions for each l, and we focus on $\gamma = 1$ here for simplicity, with other relevant values of γ yielding similar results.[28] In the case of $\gamma = 1$, the tetrahedral rotor function is given by

$$M_1 = \frac{3\sqrt{3}}{4}\sum_{i=1}^{4} x_i y_i z_i, \tag{2}$$

where $\mathbf{r}_i = (x_i, y_i, z_i)$ is a unit vector along a Br-MLWFC bond i. We then quantify the rotational motion of Br MLWFCs through the TCF,

$$C_1(t) = \frac{\langle \delta M_1(t)\delta M_1(0)\rangle}{\langle \delta M_1^2(0)\rangle}, \tag{3}$$

where $\delta M_1(t) = M_1(t) - \langle M_1\rangle$. Monitoring unit vector correlations strictly probes rotational motion of the vectors, ignoring changes in Br-MLWFC bond length, arising from changes in covalency. However, using the unnormalized Br-MLWFC vectors leads to nearly identical $C_1(t)$ correlation functions.

III. RESULTS AND DISCUSSION

The timescale for rotational motion of lone pairs can be quantified through the time correlation functions mentioned above: the Sn-LP dipole rotational correlation function and the time correlation function of the tetrahedral rotor functions for Br-LP correlations.[28] Both are shown in Fig. 2(a) for $CsSnBr_3$. These time correlation functions indicate that lone pair rotational motion of all sites occurs on timescales of several hundred femtoseconds.[28] This timescale is the same as that observed and predicted for polarization fluctuations in these materials, suggesting that lone pair rotations may be tied to these polarization fluctuations, especially those of the Sn-LP dipoles.[22] Importantly, because the Br-MLWFC rotations involve changes in Br covalency, the decay of $C_{\gamma=1}(t)$ includes any bond breaking and therefore places an upper bound on this timescale.

The prediction of rapid reorientational motion of dipolar cations suggests that many of the concepts developed for dipolar organic cation-containing perovskites can be extended to those containing a dipolar B-site cation, except that the dipole is more dynamic (its magnitude fluctuates more easily) and its rotational motion is faster. Moreover, perovskites that contain two dipolar species, such as $MAPbBr_3$, will create additional local static and dynamic correlations due to the interactions between MA^+ and Pb^{2+}-LP dipoles.[25] We suggest that the Sn-LP dipoles are connected to many of the favorable screening characteristics of $CsSnX_3$ and similar perovskites and can be examined in a manner similar to permanent MA^+ dipoles.[14,15,22,38]

The electronic plastic crystal motions in halide perovskites have implications for understanding thermal fluctuations in the electronic structure. Previous work has shown that off-centering of Sn ions widens the bandgap of $CsSnBr_3$.[24] Thus, one may anticipate that translational and rotational fluctuations of the Sn^{2+}-LP dipole, as well as the Br MLWFCs, will lead to fluctuations in the bandgap,

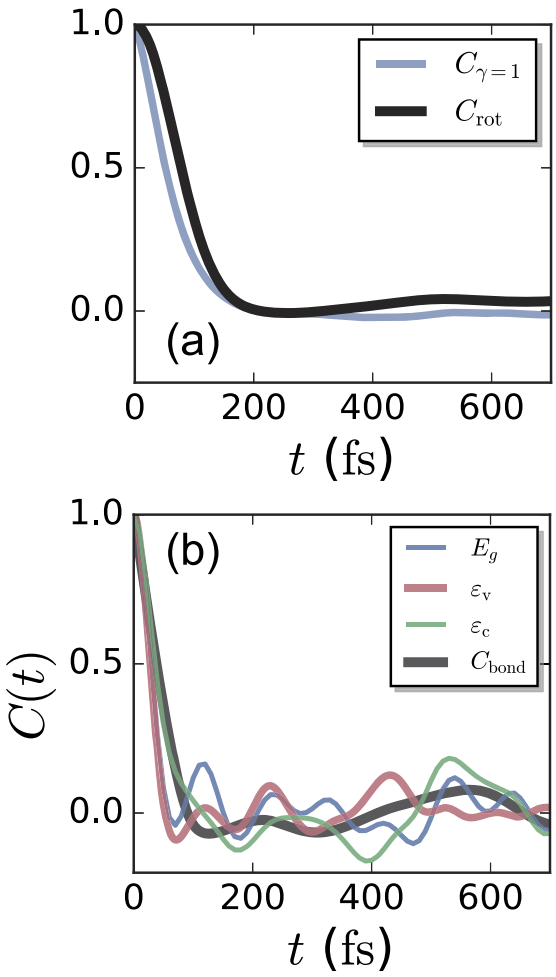

FIG. 2. (a) Time correlation functions characterizing rotational dynamics of Sn-LP [$C_{\mathrm{rot}}(t)$] and Br-MLWFC [$C_{\gamma=1}(t)$], where the latter is the time correlation function of a tetrahedral rotor function appropriate for the tetrahedral MLWFC structure around Br sites. (b) Time correlation functions of the bandgap energy fluctuations, as well as fluctuations of the conduction and valence band energy eigenvalues. The thick line corresponds to the time correlation function for strong Sn–Br covalent bonds, $C_{\mathrm{bond}}(t)$.

creating a distribution of energies at which $CsSnBr_3$ can be excited. Additionally, the top of the valence band of $CsSnBr_3$ is dominated by contributions from Br.[39–41] Therefore, we expect that fluctuations in the valence band energy will arise from fluctuations in the electronic structure of Br[42] such that the decay of the MLWFC rotational correlations will occur on timescales similar to those characterizing valence band energy fluctuations. Similar, arguments hold for fluctuations in the conduction band energy because the bottom of the conduction band is also dominated by the B-site metal orbitals.[39–41]

We can quantify the timescale for valence band fluctuations through the decay of the time correlation function,

$$C_v(t) = \frac{\langle \delta\varepsilon_v(t)\delta\varepsilon_v(0)\rangle}{\langle \delta\varepsilon_v^2\rangle}, \tag{4}$$

where $\delta\varepsilon_v(t) = \varepsilon_v(t) - \langle\varepsilon_v\rangle$ and $\varepsilon_v(t)$ is the energy eigenvalue of the valence band at time t. We also define analogous time correlation functions for the conduction band energy eigenvalue, $\varepsilon_c(t)$, and the bandgap, E_g. These time correlation functions are shown in Fig. 2(b) and decay on a similar but slightly faster timescale than the electronic rotational motion of the lone pairs. This faster decay may be expected based on the sensitivity of the valence and conduction band energies to changes in the covalency of Br atoms. As mentioned above, the decay of $C_\gamma(t)$ places an upper limit on Sn–Br bond lifetimes. Therefore, the faster decays of $C_v(t)$, $C_c(t)$, and $C_{E_g}(t)$ are consistent with Br exhibiting changes in covalency on a timescale less than the rotational timescales.

To further this perspective we examine time correlations of Sn–Br covalent bonds by monitoring nuclei–nuclei and nuclei-MLWFC correlations, following recent work.[28,43–45] We focus on strongly covalent bonds, consistent with relatively short Sn–Br bond lengths in the perovskite. Thus, we define a covalent bond to exist between a Sn–Br pair when the Sn–Br distance is less than 2.75 Å, the Sn-MLWFC (of Br) distance is less than 2.4 Å, and the Sn–Br-MLWFC angle is less than 20°. The linear Sn–Br-MLWFC angle is consistent with an electron pair located between the Sn and Br atoms, while the Sn-MLWFC distance cutoff excludes Br lone pairs, which are further from the Sn site due to increased localization on the Br atom [see Fig. 1(b) for an illustration]. We then define an indicator function, $h(t)$, which is equal to one when an Sn–Br bond exists at time t and zero otherwise. Finally, the lifetime of strong Sn–Br covalent bonds can be monitored through the time correlation function,

$$C_{\text{bond}}(t) = \frac{\langle \delta h(t)\delta h(0)\rangle}{\langle \delta h^2(0)\rangle}, \tag{5}$$

where $\delta h(t) = h(t) - \langle h(t)\rangle$. The time correlation function $C_{\text{bond}}(t)$ is also shown in Fig. 2(b) and decays on the same timescale as the electronic structure fluctuations. This suggests that the valence and conduction band fluctuations are indeed dominated by changes in Br covalency. We note that including increasingly weaker Sn–Br bonds in $C_{\text{bond}}(t)$, by extending the Sn–Br cutoff distance, increases the decay time, spanning that shown in Fig. 2(b) to that for $C_{\text{rot}}(t)$ and $C_\gamma(t)$, when the weakest bonds are included.

IV. CONCLUSIONS

In this Perspective, we suggest that localized lone pair electrons in metal halide perovskites exhibit rotational motion analogous to nuclear motions in molecular plastic crystals. We expect that these electronic plastic crystal dynamics can be observed in synchrotron measurements of the fluctuating charge density,[46–49] as well as spectroscopic methods that can probe dynamics on femtosecond timescales.[50,51] The rotational dynamics are tied to fluctuations of the electronic band energies through changes in Br covalency coupled to MLWFC rotations, with the timescale for fluctuations in valence band, conduction band, and bandgap energies being slightly faster than those for the electronic rotational dynamics. Indeed, the valence and conduction band are dominated by Br and Sn states, respectively,[41] and the dynamics of their electronic structure will impact time-dependent fluctuations of the band energies.

Our perspective on the local electronic structure and dynamics in metal halide perovskites may aid in understanding photophysical and photochemical properties of these materials. For organic–inorganic hybrid perovskites, characterization of the structural and dynamic properties of dipolar organic cations has led to significant advances in our understanding of the favorable properties of these materials.[1–3,6–17] We expect that similar qualitative understanding can be developed by generalizing these insights to dipolar metal cations, such as Sn^{2+}, in halide perovskites.

The ability of lone pair electrons to rotate at finite temperature in response to polarization fluctuations may also be relevant for understanding the surface chemistry of materials. At perovskite surfaces, lone pair sites can be exposed.[52,53] Rotational dynamics of these lone pairs could impact the structure of a perovskite interface (with a liquid, for example) and the corresponding interfacial chemistry.

We close by noting that this perspective on lone pair dynamics is not limited to halide perovskites, and we expect electronic plastic crystal motion of lone pairs to be prevalent in solids with localized lone pair electrons at finite temperatures. For example, we have predicted that these charge fluctuations should exist in halide crystals,[28] and future work will generalize these ideas to additional halide-containing solids.

ACKNOWLEDGMENTS

This work was supported as part of the Center for Complex Materials from First Principles, an Energy Frontier Research Center funded by the U.S. Department of Energy, Office of Science, Basic Energy Sciences, under Award No. DE-SC0012575. Computational resources were supported, in part, by the National Science Foundation through major research instrumentation Grant No. 1625061 and by the U.S. ARL under Contract No. W911NF-16-2-0189. We thank Ram Seshadri, Umesh Waghmare, and Tony Cheetham for useful discussions and generously sharing their thoughts and work on this subject.

DATA AVAILABILITY

The data that support the findings of this study are available within the article. Raw data files are available from the corresponding author upon reasonable request.

REFERENCES

[1] W. Li, Z. Wang, F. Deschler, S. Gao, R. H. Friend, and A. K. Cheetham, "Chemically diverse and multifunctional hybrid organic–inorganic perovskites," Nat. Rev. Mater. **2**, 16099 (2017).

[2] Y. Fu, H. Zhu, J. Chen, M. P. Hautzinger, X.-Y. Zhu, and S. Jin, "Metal halide perovskite nanostructures for optoelectronic applications and the study of physical properties," Nat. Rev. Mater. **4**, 169–188 (2019).

[3] K. Wang, D. Yang, C. Wu, M. Sanghadasa, and S. Priya, "Recent progress in fundamental understanding of halide perovskite semiconductors," Prog. Mater. Sci. **106**, 100580 (2019).

[4] L.-Y. Huang and W. R. L. Lambrecht, "Electronic band structure, phonons, and exciton binding energies of halide perovskites $CsSnCl_3$, $CsSnBr_3$, and $CsSnI_3$," Phys. Rev. B **88**, 165203 (2013).

[5] G. Li, F. W. R. Rivarola, N. J. L. K. Davis, S. Bai, T. C. Jellicoe, F. de la Peña, S. Hou, C. Ducati, F. Gao, R. H. Friend, N. C. Greenham, and Z.-K. Tan, "Highly efficient perovskite nanocrystal light-emitting diodes enabled by a universal crosslinking method," Adv. Mater. **28**, 3528–3534 (2016).

[6] A. Walsh, "Principles of chemical bonding and band gap engineering in hybrid organic–inorganic halide perovskites," J. Phys. Chem. C **119**, 5755–5760 (2015).

[7] A. A. Bakulin, O. Selig, H. J. Bakker, Y. L. Rezus, C. Müller, T. Glaser, R. Lovrincic, Z. Sun, Z. Chen, A. Walsh *et al.*, "Real-time observation of organic cation reorientation in methylammonium lead iodide perovskites," J. Phys. Chem. Lett. **6**, 3663–3669 (2015).

[8] A. M. A. Leguy, J. M. Frost, A. P. McMahon, V. G. Sakai, W. Kockelmann, C. Law, X. Li, F. Foglia, A. Walsh, B. C. O'Regan *et al.*, "The dynamics of methylammonium ions in hybrid organic–inorganic perovskite solar cells," Nat. Commun. **6**, 7124 (2015).

[9] M. A. Carignano, A. Kachmar, and J. Hutter, "Thermal effects on $CH_3NH_3PbI_3$ perovskite from *ab initio* molecular dynamics simulations," J. Phys. Chem. C **119**, 8991–8997 (2015).

[10] D. H. Fabini, T. A. Siaw, C. C. Stoumpos, G. Laurita, D. Olds, K. Page, J. G. Hu, M. G. Kanatzidis, S. Han, and R. Seshadri, "Universal dynamics of molecular reorientation in hybrid lead iodide perovskites," J. Am. Chem. Soc. **139**, 16875–16884 (2017).

[11] C. G. Bischak, C. L. Hetherington, H. Wu, S. Aloni, D. F. Ogletree, D. T. Limmer, and N. S. Ginsberg, "Origin of reversible photoinduced phase separation in hybrid perovskites," Nano Lett. **17**, 1028–1033 (2017).

[12] D. A. Egger, A. M. Rappe, and L. Kronik, "Hybrid organic–inorganic perovskites on the move," Acc. Chem. Res. **49**, 573–581 (2016).

[13] X. Y. Zhu and V. Podzorov, "Charge carriers in hybrid organic–inorganic lead halide perovskites might be protected as large polarons," J. Phys. Chem. Lett. **6**, 4758–4761 (2015).

[14] H. Zhu, K. Miyata, Y. Fu, J. Wang, P. P. Joshi, D. Niesner, K. W. Williams, S. Jin, and X. Y. Zhu, "Screening in crystalline liquids protects energetic carriers in hybrid perovskites," Science **353**, 1409–1413 (2016).

[15] K. Miyata, T. L. Atallah, and X.-Y. Zhu, "Lead halide perovskites: Crystal-liquid duality, phonon glass electron crystals, and large polaron formation," Sci. Adv. **3**, e1701469 (2017).

[16] M. Lai, A. Obliger, D. Lu, C. S. Kley, C. G. Bischak, Q. Kong, T. Lei, L. Dou, N. S. Ginsberg, D. T. Limmer *et al.*, "Intrinsic anion diffusivity in lead halide perovskites is facilitated by a soft lattice," Proc. Natl. Acad. Sci. U. S. A. **115**, 11929–11934 (2018).

[17] Y. Guo, O. Yaffe, T. D. Hull, J. S. Owen, D. R. Reichman, and L. E. Brus, "Dynamic emission Stokes shift and liquid-like dielectric solvation of band edge carriers in lead-halide perovskites," Nat. Commun. **10**, 1175 (2019).

[18] M. Kulbak, D. Cahen, and G. Hodes, "How important is the organic part of lead halide perovskite photovoltaic cells? Efficient $CsPbBr_3$ cells," J. Phys. Chem. Lett. **6**, 2452–2456 (2015).

[19] G. E. Eperon, G. M. Paternò, R. J. Sutton, A. Zampetti, A. A. Haghighirad, F. Cacialli, and H. J. Snaith, "Inorganic caesium lead iodide perovskite solar cells," J. Mater. Chem. A **3**, 19688–19695 (2015).

[20] S. Gupta, T. Bendikov, G. Hodes, and D. Cahen, "$CsSnBr_3$, a lead-free halide perovskite for long-term solar cell application: Insights on SnF_2 addition," ACS Energy Lett. **1**, 1028–1033 (2016).

[21] E. M. Hutter, R. J. Sutton, S. Chandrashekar, M. Abdi-Jalebi, S. D. Stranks, H. J. Snaith, and T. J. Savenije, "Vapour-deposited cesium lead iodide perovskites: Microsecond charge carrier lifetimes and enhanced photovoltaic performance," ACS Energy Lett. **2**, 1901–1908 (2017).

[22] O. Yaffe, Y. Guo, L. Z. Tan, D. A. Egger, T. Hull, C. C. Stoumpos, F. Zheng, T. F. Heinz, L. Kronik, M. G. Kanatzidis, J. S. Owen, A. M. Rappe, M. A. Pimenta, and L. E. Brus, "Local polar fluctuations in lead halide perovskite crystals," Phys. Rev. Lett. **118**, 136001 (2017).

[23] U. V. Waghmare, N. A. Spaldin, H. C. Kandpal, and R. Seshadri, "First-principles indicators of metallicity and cation off-centricity in the IV-VI rocksalt chalcogenides of divalent Ge, Sn, and Pb," Phys. Rev. B **67**, 125111 (2003).

[24] D. H. Fabini, G. Laurita, J. S. Bechtel, C. C. Stoumpos, H. A. Evans, A. G. Kontos, Y. S. Raptis, P. Falaras, A. Van der Ven, M. G. Kanatzidis, and R. Seshadri, "Dynamic stereochemical activity of the Sn^{2+} lone pair in perovskite $CsSnBr_3$," J. Am. Chem. Soc. **138**, 11820–11832 (2016).

[25] G. Laurita, D. H. Fabini, C. C. Stoumpos, M. G. Kanatzidis, and R. Seshadri, "Chemical tuning of dynamic cation off-centering in the cubic phases of hybrid tin and lead halide perovskites," Chem. Sci. **8**, 5628–5635 (2017).

[26] A. N. Beecher, O. E. Semonin, J. M. Skelton, J. M. Frost, M. W. Terban, H. Zhai, A. Alatas, J. S. Owen, A. Walsh, and S. J. L. Billinge, "Direct observation of dynamic symmetry breaking above room temperature in methylammonium lead iodide perovskite," ACS Energy Lett. **1**, 880–887 (2016).

[27] S. K. Radha, C. Bhandari, and W. R. L. Lambrecht, "Distortion modes in halide perovskites: To twist or to stretch, a matter of tolerance and lone pairs," Phys. Rev. Mater. **2**, 063605 (2018).

[28] R. C. Remsing and M. L. Klein, "Lone pair rotational dynamics in solids," Phys. Rev. Lett. **124**, 066001 (2020).

[29] M. L. Klein, I. R. McDonald, and Y. Ozaki, "Orientational order in ionic crystals containing tetrahedral ions," J. Chem. Phys. **79**, 5579–5587 (1983).

[30] M. L. Klein and L. J. Lewis, "Simulation of dynamical processes in molecular solids," Chem. Rev. **90**, 459–479 (1990).

[31] J. VandeVondele, M. Krack, F. Mohamed, M. Parrinello, T. Chassaing, and J. Hutter, "Quickstep: Fast and accurate density functional calculations using a mixed Gaussian and plane waves approach," Comput. Phys. Commun. **167**, 103–128 (2005).

[32] J. VandeVondele and J. Hutter, "Gaussian basis sets for accurate calculations on molecular systems in gas and condensed phases," J. Chem. Phys. **127**, 114105 (2007).

[33] S. Goedecker, M. Teter, and J. Hutter, "Separable dual-space Gaussian pseudopotentials," Phys. Rev. B **54**, 1703–1710 (1996).

[34] J. P. Perdew, K. Burke, and M. Ernzerhof, "Generalized gradient approximation made simple," Phys. Rev. Lett. **77**, 3865–3868 (1996).

[35] S. Nosé, "A unified formulation of the constant temperature molecular dynamics methods," J. Chem. Phys. **81**, 511–519 (1984).

[36] S. Nosé, "A molecular dynamics method for simulations in the canonical ensemble," Mol. Phys. **52**, 255–268 (1984).

[37] G. Berghold, C. J. Mundy, A. H. Romero, J. Hutter, and M. Parrinello, "General and efficient algorithms for obtaining maximally localized Wannier functions," Phys. Rev. B **61**, 10040–10048 (2000).

[38] M. Z. Mayers, L. Z. Tan, D. A. Egger, A. M. Rappe, and D. R. Reichman, "How lattice and charge fluctuations control carrier dynamics in halide perovskites," Nano Lett. **18**, 8041–8046 (2018).

[39] G. Murtaza and I. Ahmad, "First principle study of the structural and optoelectronic properties of cubic perovskites $CsPbM_3$ (M = Cl, Br, I)," Physica B **406**, 3222–3229 (2011).

[40] L. Protesescu, S. Yakunin, M. I. Bodnarchuk, F. Krieg, R. Caputo, C. H. Hendon, R. X. Yang, A. Walsh, and M. V. Kovalenko, "Nanocrystals of cesium lead halide perovskites ($CsPbX_3$, X = Cl, Br, and I): Novel optoelectronic materials showing bright emission with wide color gamut," Nano Lett. **15**, 3692–3696 (2015).

[41] F. G. Santomauro, J. Grilj, L. Mewes, G. Nedelcu, S. Yakunin, T. Rossi, G. Capano, A. Al Haddad, J. Budarz, D. Kinschel, D. S. Ferreira, G. Rossi, M. Gutierrez Tovar, D. Grolimund, V. Samson, M. Nachtegaal, G. Smolentsev, M. V. Kovalenko, and M. Chergui, "Localized holes and delocalized electrons in

photoexcited inorganic perovskites: Watching each atomic actor by picosecond X-ray absorption spectroscopy," Struct. Dyn. **4**, 044002 (2017).
[42]S. McKechnie, J. M. Frost, D. Pashov, P. Azarhoosh, A. Walsh, and M. van Schilfgaarde, "Dynamic symmetry breaking and spin splitting in metal halide perovskites," Phys. Rev. B **98**, 085108 (2018).
[43]R. C. Remsing and M. L. Klein, "Halogen bond structure and dynamics from molecular simulations," J. Phys. Chem. B **123**, 6266–6273 (2019).
[44]R. C. Remsing, J. Sun, U. V. Waghmare, and M. L. Klein, "Bonding in the metallic molecular solid α-gallium," Mol. Phys. **116**, 3372–3379 (2018).
[45]R. C. Remsing and M. L. Klein, "Molecular simulation of covalent bond dynamics in liquid silicon," J. Phys. Chem. B **124**, 3180–3185 (2020).
[46]S. Huotari, C. Sternemann, M. C. Troparevsky, A. G. Eguiluz, M. Volmer, H. Sternemann, H. Müller, G. Monaco, and W. Schülke, "Strong deviations from jellium behavior in the valence electron dynamics of potassium," Phys. Rev. B **80**, 155107 (2009).
[47]W. Schülke, *Electron Dynamics by Inelastic X-Ray Scattering* (Oxford University Press, New York, 2007), Vol. 7.
[48]S. R. Leone, M. Ahmed, and K. R. Wilson, "Chemical dynamics, molecular energetics, and kinetics at the synchrotron," Phys. Chem. Chem. Phys. **12**, 6564–6578 (2010).
[49]M. Dutta, K. Pal, U. V. Waghmare, and K. Biswas, "Bonding heterogeneity and lone pair induced anharmonicity resulted in ultralow thermal conductivity and promising thermoelectric properties in *n*-type $AgPbBiSe_3$," Chem. Sci. **10**, 4905–4913 (2019).
[50]K. Ramasesha, S. R. Leone, and D. M. Neumark, "Real-time probing of electron dynamics using attosecond time-resolved spectroscopy," Annu. Rev. Phys. Chem. **67**, 41–63 (2016).
[51]J. Riemensberger, S. Neppl, D. Potamianos, M. Schäffer, M. Schnitzenbaumer, M. Ossiander, C. Schröder, A. Guggenmos, U. Kleineberg, D. Menzel *et al.*, "Attosecond dynamics of sp-band photoexcitation," Phys. Rev. Lett. **123**, 176801 (2019).
[52]J. Padilla and D. Vanderbilt, "*Ab initio* study of $BaTiO_3$ surfaces," Phys. Rev. B **56**, 1625–1631 (1997).
[53]D. W. Davies, A. Walsh, J. J. Mudd, C. F. McConville, A. Regoutz, J. M. Kahk, D. J. Payne, V. R. Dhanak, D. Hesp, K. Pussi, T.-L. Lee, R. G. Egdell, and K. H. L. Zhang, "Identification of lone-pair surface states on indium oxide," J. Phys. Chem. C **123**, 1700–1709 (2019).